

A landscape of hydride compounds for off-board refilling of transport vehicles

Klaus Lieutenant^{a*}, Ana Borissova^b

^a Forschungszentrum Jülich GmbH, Wilhelm-Johnen-Straße, D-52425 Jülich, Germany

^b Faculty of Education and Arts, Nord University, Mørkvedtråkket 30, 8049 Bodø, Norway

*Corresponding author:

Email : k.lieutenant@fz-juelich.de

Phone: +49 2461 61 4706

Fax : +49 2461 61 2610

Abstract:

The authors compare the energy consumption of hydrogen cars (using fuel cells) with electric cars (using batteries) and conventional petrol cars finding that hydrogen cars are preferable to electric cars for long distances.

They evaluate several types of hydrogen storage materials in terms of off-board refilling, in which hydrogen uptake takes place outside the vehicle. Literature values for enthalpy and entropy of formation etc. are used to calculate hydrogen densities, heat production and theoretical desorption temperature. Additionally, experimental literature values for temperature and pressure of (de)hydrogenation, kinetics and cycling stability are summarized. The results are discussed assuming that hydrogen refilling takes place in a replaceable tank outside the vehicle, which reduces the DOE requirements to high volumetric and gravimetric density, moderate release temperature, sufficiently fast release and high reversibility. They are fulfilled by materials like NaAlH₄, while even better performance can be expected from compounds like LiBH₄+MeH_x or Mg-Ti composites.

Keywords: energy storage materials, hydrogen storage, mobile application, off-board refilling, energy efficiency

Highlights:

- Hydrogen cars have the lowest primary energy consumption for long cruising ranges
- Off-board refilling is the only solution for solid state hydrogen storage materials
- Off-board refilling enables short refilling times and fulfills the DOE requirements

1. Introduction

1.1 Use of renewable energies

The world energy consumption is constantly rising because the population is still growing and a rising number of people can afford buying cars, air condition, travels and various technical equipment. As most of the energy comes from burning fossil fuels, which produces the greenhouse gas carbon dioxide, the content of this gas in the atmosphere is constantly rising [1]. This is the main contribution to the climate change that the humanity experiences the last decades [2]. Progress in efficiency of various technical equipment and efforts to reduce consumption, e.g. by improved insulation, could only slow down the increase in CO₂ output.

The only way out is to strengthen the efforts to generate electricity from renewable sources and to use it as efficiently as possible. (Using nuclear energy can help during a transition period, but is not a sustainable solution. The fusion technology might solve the energy problem one day, but it is still unreachable for the short term [3].) The renewable sources that have to be utilized in the future are hydropower, solar, wind and geothermal energy. The use of hydropower is increasing slowly in many parts of the world [4], the geothermal power technology is still being developed for worldwide use [5] so that the main additional contribution in the next years are from wind energy and solar energy.

The problem is that the generation of electricity from these two sources varies with time and cannot be adapted to the actual consumption. If their contribution to the total electricity production is not too large, e.g. less than about a third, the variation can be balanced by varying the electricity generation from other sources like gas power plants. Additionally, electricity may be transported according to lack or excess of generation in different countries or regions. But this is limited by the transport capacity and the loss of electrical energy of about 1% per 100 km [6].

The closer one gets to 100% electricity generation from renewable energies, which usually means a high percentage from wind and solar energy, the more it gets necessary to have an efficient large scale energy storage system [7, 8]. This is especially true for regions above 40° latitude where solar energy is mainly available during summer, while the energy consumption is higher in winter when heating is needed, while tropical regions might come along with any kind of electrical or mechanical storage that is able to buffer day to night variations.

1.2 Hydrogen as energy carrier

So far, only two systems for storage of large amounts of energy are known: pumped storage or storage in form of chemical energy. Pumped storage is a well-established system with a quite high efficiency of 70% to 80% [9], but the resources are limited in many countries.

For chemical storage, hydrogen is one of the substances that has been suggested as energy carrier. Its advantages are (1) its high energy density of 120 MJ/kg (compared to 44 MJ/kg for petrol) [10], (2) the fact that only water is produced when it is used and (3) its flexibility - it can be produced from various sources and used for combustion or electricity generation.

When more electrical energy is generated than used, hydrogen could be produced. It can then be used at any time by industry, for transport or heating. For the stationary storage of hydrogen several solutions are suggested [11]. In densely populated areas, it seems to be the best solution to store it directly inside a pipeline network (at moderate pressures) [12]; alternatively, caverns or large tanks could be used. Liquefaction or high pressure gas storage need a lot of energy and are therefore unfavorable [13] .

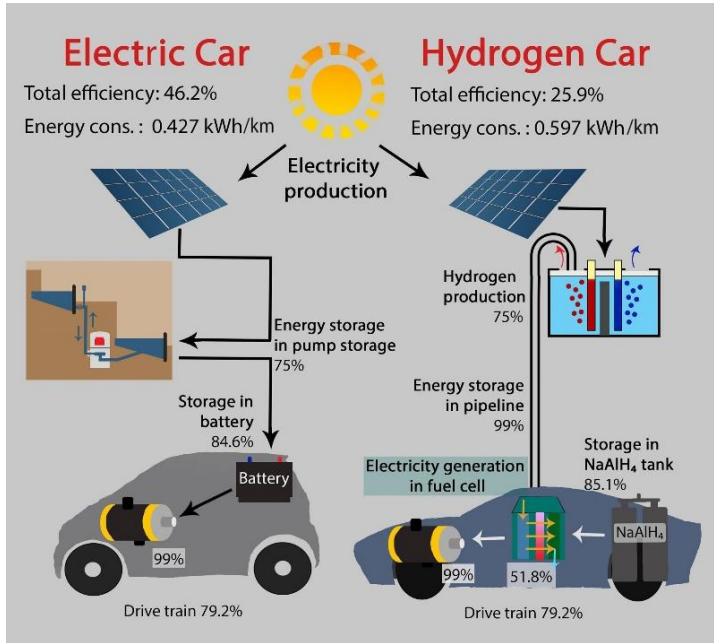
1.3 Hydrogen vehicles and electrical vehicles

While the use of renewable energy in various areas is rising, mainly via a rising percentage of electricity generated from renewable sources, the transport is still dominated by cars driven by fossil fuels. Electric cars are available, but not yet widely used, though they are energy efficient. Apart from the high price, the long charging times and the short cruising range are the problems. The reason for the latter is the low energy density of the batteries, which requires large and heavy batteries for a proper driving range. Li-ion batteries have at present the highest energy density of 0.875 MJ/kg [6] which results in a battery mass of at least 100 kg per 100 km range. So it works fine for a city car, but it cannot well be used for long distances.

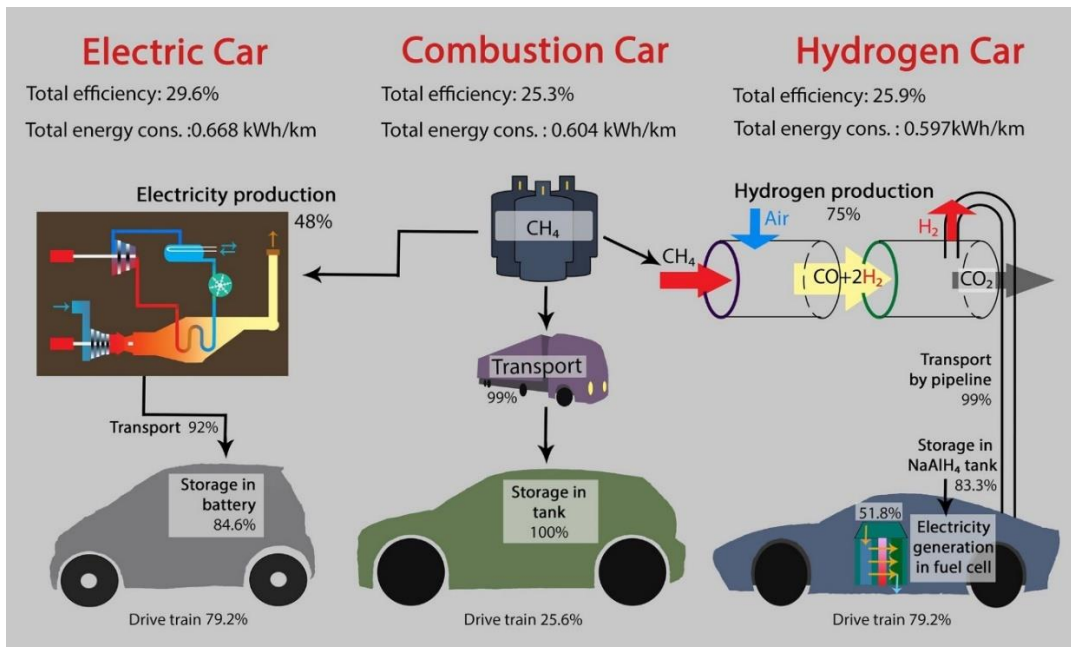
The energy density of a hydrogen tank can be much higher. Therefore, a hydrogen car is an alternative to the electrical car, especially for cars meant to be used for long distances. In addition, refilling can be much faster (see below). So a hydrogen car is probably easier accepted by customers as a car needed for long range driving.

Hydrogen cars usually use electric motors. (Combustion of hydrogen is also possible, but less efficient.) The electricity is generated by a fuel cell. If the hydrogen is generated from electricity, hydrogen cars have a lower overall efficiency than electric cars, because of the two transformations from electricity to hydrogen and back, which both have a limited efficiency (cf. Fig. 1a, Table 1, Appendix 1). However, a wide use of electric cars with electricity

generated from renewable sources, only works well if a high fraction of the electricity is generated in hydropower plants or a large storage capacity in pumped storage power stations is available; otherwise electricity consumption and generation cannot be matched.



(a)



(b)

Fig. 1: Performance comparison of different propulsion systems

Comparison of total efficiencies and energy consumptions of electrical car, hydrogen car and combustion car using electricity (a) and methane (b) as primary energy source for cars of 500 km cruising range considering effects of different masses of motor, battery and tank (cf. Table 1b, Appendix 1).

Nowadays, there is not enough electricity generated from renewable sources for all possible applications. Additional applications require therefore the generation from hydrocarbons. This electricity can be used to run cars; or the hydrocarbons are used to produce hydrogen (to run cars) or it is directly used in a car. These options are illustrated in Figure 1 and compared in Table 1.

The data in Table 1a show that an electric car using a Li battery works clearly most efficient for short distances. However, this calculation leaves out the fact that the production of a battery car causes at least twice the amount of CO₂ emission than that of a normal car (or a hydrogen car) because of its large battery [14, 15]. This means that a real gain is reached only after a long driving distance (130000 km or more depending on the size of battery and car, conditions of electricity generation and battery construction etc.). It also does not consider additional consumption for heating the interior of the car during winter, because waste heat from engine or fuel cell, which is used in other types of cars, is not available.

In addition, the mass of the battery becomes more and more of a problem with increasing cruising range. It requires a stronger engine and a more solid chassis, which both increase the weight and the consumption. This requires an even larger battery, which again results in a heavier car and so on. This effect was already described earlier and the mass of the car calculated as a function of driving range for different kinds of batteries in a battery electric vehicles (BEV) and for fuel cell electric vehicles (FCEV) [6].

This kind of calculation is repeated here to determine the total energy consumption using many of the parameters given there. We do this for a hypothetical car, medium sized car of equipped with different kinds of engines, which has 1200 kg net weight (with full tank) as a petrol car. The idea is to investigate principal properties, not to evaluate existing cars, especially differences between cars made for short and long distances. Therefore, we have chosen a very short cruising range of only 150 km (for a city car) and a long one of 500 km (for a long distance car).

We followed the idea from [6] to keep the ratio between power and mass fixed to enable constant acceleration and climbing ability. We also used several factors from that publication, but not all numbers needed to calculate the car masses were given there, so that we had to determine or estimate some of them. They might be wrong by some percent, but this will not significantly alter the result, because the main effect is the increasing battery weight. All number are listed in Appendix 1:

1. The energy densities are taken from the literature (see Appendix 1)

2. The efficiency ϵ_{car} inside the car is the efficiency of the complete propulsion system, for cars with electric motor times the efficiency of the fuel cell or of discharging the battery (see also Appendix 1)
3. The total efficiency ϵ_{tot} includes additionally (where applicable): transport, conversion and processing (charging, compression, chemical reaction)

$$\epsilon_{\text{tot}} = \epsilon_{\text{car}} \cdot \epsilon_{\text{trans}} \cdot \epsilon_{\text{conv}} \cdot \epsilon_{\text{proc}}$$

4. For the city car, a cruising range of 150 km is assumed, for the long distance car, a range of 500 km. The large difference is chosen to bring out the principal differences between these two types of cars.
5. It is assumed that the mass m_{base} of chassis plus vehicle body increases with total car weight. Assuming that the linear part is 15% of the total mass and a total mass of $m_{\text{tot}} = 1200$ kg for the petrol car (s.a, Table 1b), we get the base mass $m_{\text{base},0}$

$$m_{\text{base},0} = m_{\text{tot}} - 0.15 m_{\text{tot}} - m_{\text{motor}} - m_{\text{fuel}} - m_{\text{tank}} - m_{\text{FC+batt}} = 735 \text{ kg}$$

and thus the equation for the mass of chassis plus superstructure:

$$m_{\text{base}} = m_{\text{base},0} + 0.15 m_{\text{tot}}$$

to reach the planned total mass of 1200 kg of the petrol car (see Table 1b).

6. The mass m_{motor} of the propulsion system is assumed to be proportional to the power of the motor with the following factors: 4 kg/kW for a combustion engine and 2 kg/kW for an electric motor.
7. The battery of a normal car weighs about 15 kg (0.72 kWh, measured), the one for a FCEV is supposed to be somewhat heavier, 20 kg (corresponding to 1 kWh for a lead battery and 17.5 kWh for Li-ion battery). The battery of a battery electric car is by far heavier. Its mass is determined by the energy E_{tot} needed for the wanted cruising range, the energy density available ($\rho_{\text{E,Li}} = 0.875 \text{ MJ/kg} = 0.243 \text{ kWh/kg}$ for L-ion batteries), and the fraction $\kappa = 0.7$ [6] of the battery charge that is available:

$$m_{\text{batt,BC}} = E_{\text{tot}} / \rho_{\text{E,Li}} \cdot 1/\kappa$$

8. The mass of the fuel cell is assumed to be proportional to the power; a recently produced cell had a factor of 0.694 kg/kW [16].
9. The masses of the tanks (including additional devices like control and discharging systems) are also assumed to be proportional to the amount of fuel:

$$m_{\text{tank}} = K m_{\text{fuel}}$$

using $K_{\text{CH}_4} = 5.0$, $K_{\text{CGH}_2} = 16.5$ [17], $K_{\text{NaAlH}_4} = 20.0$. Only for petrol a fixed mass of 7 kg is assumed.

10. The total mass m_{tot} is the sum of the five masses described.

11. The power P_{mot} is set proportional to the to car mass

$$P_{\text{mot}} = 0.05 \text{ kW/kg} \cdot m_{\text{tot}}$$

12. The energy consumption increases with the total mass of the car

$$C/C_0 = (m_{\text{tot}}/m_{\text{tot},0})^{0.6}$$

[6]. The standard mass $m_{\text{tot},0}$ is set to 1200 kg and the standard energy consumption to $C_0 = 6 \text{ L/(100 km)}$ corresponding to

$$c_0 = C_0/100 \rho_{\text{petrol}} \rho_{E,\text{petrol}} / 3.6 \text{ kWh/MJ} = 0.557 \text{ kWh/km}$$

giving the energy consumption at the wheels

$$C_{0,\text{wheel}} = C_0 \cdot \epsilon_{\text{car,petrol}} = 0.143 \text{ kWh/km}$$

and

$$c = c_0 \cdot (m_{\text{tot}}/m_{\text{tot},0})^{0.6}$$

13. This allows calculating the primary energy consumption needed

$$C_{0,\text{tot}} = C_{0,\text{wheel}} / \epsilon_{\text{tot}}$$

The calculated values of the motor power P_{mot} is used to calculate the new motor and fuel cell mass. The calculated consumption is used to calculate the new fuel, tank and battery mass. The calculated car mass is used to calculate the new base mass. This gives a new total mass leading to a new motor power and a new consumption. This procedure is repeated until it has converged.

Fuel	P_{mot} [kW]	Cons. at wheel [kWh/km]	Energy density [MJ/kg]	Efficiency in car	m_{base} [kg]	m_{motor} [kg]	$m_{\text{FC+batt}}$ [kg]	m_{fuel} [kg]	$m_{\text{tank+BOP}}$ [kg]	m_{tot} [kg]	Total efficiency from electricity	Total consumption from electricity [kWh/km]	Total efficiency from methane	Total consumption from methane [kWh/km]
petrol	58.8	0.141	44.0	0.256	911	235	15	6.8	7	1175				
methane	60.4	0.143	50.0	0.256	916	242	15	6.0	30	1208			0.253	0.565
Li battery	60.9	0.144	0.9	0.713	918	122	178			1218	0.616	0.234	0.296	0.487
H ₂ gas	58.3	0.140	120.0	0.410	910	117	104	1.5	34	1166	0.256	0.548	0.256	0.548
NaAlH ₄	61.9	0.145	120.0	0.410	913	119	106	1.6	47	1186	0.259	0.547	0.259	0.547

Table 1a: Energy consumption (without any pumped storage losses) of a medium sized city car of cruising range 150 km using different propulsion systems. Efficiencies and total energy consumption are calculated for electricity and methane as primary energy sources (details see text, cf. Appendix 1)

Fuel	Power [kW]	Cons. at wheel [kWh/km]	Energy density [MJ/kg]	Efficiency in car	m_{base} [kg]	m_{motor} [kg]	$m_{\text{FC+batt}}$ [kg]	m_{fuel} [kg]	$m_{\text{tank+BOP}}$ [kg]	m_{tot} [kg]	Total efficiency from electricity	Total consumption from electricity [kWh/km]	Total efficiency from methane	Total consumption from methane [kWh/km]
petrol	60.0	0.143	44.0	0.256	915	240	15	22.8	7	1200				
methane	67.4	0.153	50.0	0.256	937	270	15	21.4	105	1349			0.253	0.604
Li battery	103.3	0.198	0.9	0.713	1045	207	815			2066	0.462	0.427	0.296	0.668
H ₂ gas	62.7	0.146	120.0	0.410	923	125	111	5.4	88	1253	0.256	0.572	0.256	0.572
NaAlH ₄	68.5	0.155	120.0	0.410	941	137	119	5.7	170	1373	0.259	0.597	0.259	0.597

Table 1b: Energy consumption of a medium sized long distance car of cruising range 500 km using different propulsion systems. Efficiencies and total energy consumption are calculated for electricity and methane as primary energy sources. The calculation assumes increased motor power to compensate increased weight because of a large tank or battery and losses by pumped storage for electricity generation (details see text, cf. Fig. 1, Appendix 1)

The result of this procedure is shown in Table 1 for two cruising ranges of 150 km and 500 km: For up to 150 km, the masses of all cars are rather similar (s. Table 1a). The heavier tank of the cars driven by an electric motor is compensated by the lighter motor. As a consequence, the electric car has the lowest energy consumption due to the high efficiency of its propulsion system and its energy conversion.

However, for a cruising range of 500 km, the situation looks different: Starting from about 1200 kg, the mass of the BEV has increased to over 2000 kg caused by a battery of over 800

kg. As a consequence, the consumption at wheel has increased by 37.3%. If electricity from natural sources is available, then this is still the most efficient car, even if loss by energy storage, e.g. in a pumped storage power station is considered as in Table 1b, because an electric motor is so much more efficient than a combustion engine and the energy conversion from electricity to hydrogen and back reduces the efficiency of the hydrogen car. But if the electricity is generated from hydrocarbons, then the electric car shows the highest consumption of primary energy (see Table 1b). Under these conditions, the hydrogen car has the lowest energy consumption in spite of the twofold energy conversion from methane to hydrogen and from hydrogen to electricity, because the car is rather light and the motor works with high efficiency. A similar calculation using somewhat different numbers by Thomas [6], who compared cars with electric motors, using different batteries with those using hydrogen fuel cells, gave similar results. The advantage for fuel cells was even larger.

The resulting numbers depend on the factors assumed, but the overall result is always the same. If we assume the proportional part of m_{base} to be 10% (20%) of the total mass, the battery car has a total mass of 1990 (2159) kg and a consumption of 0.653 (0.686) kWh/km compared to 2066 kg and 0.668 kWh/kg calculated for 15%. All other results do not significantly change.

The driving range, on the other hand is crucial. While the electric car has about the same total mass as the other cars for the 150 km chosen, has only 10 to 64 kg higher mass than the other cars, the difference increases to 83 to 144 kg for 200 km.

Summarizing, an electric city car run on battery is unbeatable; but an electric car made for long distances becomes necessarily very heavy with existing battery technology. So a small car running on batteries for long distances cannot be built. In contrast, long distance cars running on fuel cells can have about the same mass as a conventional combustion cars and therefore retain a good energy efficiency.

The calculation also shows that reducing the weight of the tank by an improved hydrogen storage system still has a significant effect on the energy efficiency (cf. last two lines in Table 1b). Therefore, searching for better hydrogen storage materials still makes sense - for a higher safety and for a better energy efficiency.

Combined with the approach to produce hydrogen at times of excess of renewable energy, hydrogen is a good solution in addition to the electric car.

Another solution is a combination of electric and hydrogen car. As most hydrogen cars have anyway a battery to regain the kinetic energy that is lost during braking, a larger battery that

allows short distance driving and a hydrogen tank for long distances would be the ideal combination, both in terms of fuel efficiency and practicability.

As electric motors supplied by batteries are best suited for vehicles used for small distances, it is clear that for vehicles like trucks, busses or ferryboats it is a much better choice to use hydrogen as energy source.

1.4 Hydrogen storage and off-board hydrogenation.

The three main ways to store hydrogen in a compact form are: hydrogen gas under high pressure, liquid hydrogen at -253°C and hydrogen in chemical compounds in solid state form. Most of the hydrogen cars produced, both prototypes and production cars, use the first storage method: gas in high-pressure tanks (of up to 700 bar) inside the car. One possible explanation why this method is preferred by car producers is that it allows easy and fast refilling of the hydrogen container inside the vehicle. On-board refilling meets the customers' expectations. The solid state hydrogen storage materials, although they offer better security, a higher volumetric density and, if the tank is included, even higher gravimetric density than compressed gas (see Table 2), are still not in favorable position for application purposes due to disadvantageous material properties like slow reaction kinetics or high temperature and/or pressure needed for the re-hydrogenation process (see Table 3). A solution for solid state hydrogen materials utilization may appear by implementation of a changeable container, where recharging of the tank can take place outside the vehicle. Løvvik discussed this way of applying solid state materials for hydrogen storage in cars [18]. The author elucidates the idea in terms of using the heat excess for high-temperature electrolysis, which appears to be a more efficient hydrogen production method than hydrolysis [19].

In the present article, important parameters like heat excess, volumetric and gravimetric density are calculated for the corresponding hydride systems in order to evaluate the possible use of the materials in off-board and on-board refilling.

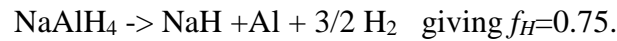
2. Thermodynamics of different hydrogen storage systems

In order to determine whether the hydrogen storage properties of the materials are appropriate for refilling outside the vehicle, several parameters were determined. The basic properties are taken from literature in order to calculate the rest of the parameters. It is assumed that 5 kg of hydrogen are needed.

If one uses the known numbers for energy content of hydrogen and petrol, the density of petrol, efficiencies of 32% for a petrol engine and 99% for an electric motor, the same losses (of 20%) in the propulsion system and an efficiency of 51.8% of the fuel cell [6, 20], it can be calculated that this corresponds to 28.8 liters of fuel in a petrol car (cf. Table 1, Appendix 1), which would be sufficient to go 480 for a consumption of 6 L/100 km.

The density ρ of each material as well as the values of the standard enthalpies and entropies of formation ΔH_f and ΔS_f of reactants and products are taken from the literature. Based on that, the calculations of the various parameters were performed by using the following theoretical approaches and formulae:

1. The fraction of the H-atoms released f_H was calculated from the stoichiometric ratio considering that in some cases a part of the hydrogen atoms are left in the system for the foreseen desorption temperature, because LiH and NaH are chemically stable. As an example, NaAlH₄ releases only 3 of the 4 hydrogen atoms at temperatures usable for fuel PEM fuel cell applications,[10]:



2. The gravimetric density (mass%) is calculated by taking the H-atoms fraction release f_H multiplied by the number of hydrogen atoms n and atomic weight of hydrogen $A_w(H)$ in a compound and divided by the molecular weight of the corresponding hydride $M_w(\text{hydride})$

$$\text{mass}\% = \frac{f_H n A_w(H)}{M_w(\text{hydride})}$$

3. The energy density ρ_E was calculated by multiplying the gravimetric density $\text{mass}\%$ with the energy density of hydrogen ρ_{E,H_2} :

$$\rho_E = \text{mass}\% \rho_{E,H_2}$$

4. The volumetric hydrogen density ρ_V is calculated by multiplying the gravimetric hydrogen density $\text{mass}\%$ with the density ρ of the material.

$$\rho_V = \text{mass\%} \cdot \rho$$

5. The heat production in units of [MJ] is calculated by:

$$Q = \frac{\Delta H \cdot m}{M_w(H_2)}$$

where ΔH is the enthalpy of formation for every hydride, or, more general, the difference in enthalpy of formation between products and reactants. $M_w(H_2)$ is the molecular weight of hydrogen gas and m is the mass of the hydrogen gas (5 kg).

6. The energy loss (in %) is calculated by using the following equation

$$E_{loss}(\%) = \frac{Q}{\rho_{E,H_2} \cdot m} = \frac{\Delta H}{\rho_{E,H_2} \cdot M_w(H_2)}$$

Q is the heat production in [MJ], ρ_{E,H_2} is the energy density of hydrogen (120 MJ/kg) and m is the mass of the hydride (5 kg).

7. The evaporation heat of nitrogen [MJ/kg] is calculated by dividing the heat of evaporation of N_2 , 5.58 kJ per mol [21], by the molecular weight of nitrogen giving $q_{evap}=0.199$ MJ/kg N_2 , which allows to calculate the necessary mass of nitrogen m_{comp} in [kg N_2] to compensate the produced heat of hydrogen absorption Q_{prod} :

$$m_{comp} = \frac{Q_{prod}}{q_{evap}}$$

8. The Van't Hoff equation

$$\ln\left(\frac{p}{p_0}\right) = \frac{\Delta H}{RT} - \frac{\Delta S}{R}$$

is used in order to calculate the theoretical desorption temperature at equilibrium pressure of $p = 1$ bar and the theoretical pressure at 25°C. p_0 is the standard pressure, and p is the pressure at any temperature.

Material	Fraction	Gravimetric density	Energy density	Volumetric density	ρ [kg/L]	m [kg]	V [m ³]	ΔH [kJ/mol]	ΔS [J/(mol K)]	Energy loss	Heat production	Heat compensation	T (1 bar)	p(T0) [bar]	References
DOE Target 2015		5.50 %		40.0											[22]
GH ₂ , 700 bar	1.00	100%	120.0	37.0		5.0	0.135			15.0%					[13]
with tank	1.00	5.72 %	6.9	26.7		87.4	0.187								[12, 13], [17, 23]
LH ₂ , -253°C	1.00	100%	120.0	70.8		5.0	0.071	-0.9		30.0%	-2.2	16	-253	4.3E+06	[10, 13]
with tank	1.00	14.47 %	17.4	50.6		34.6	0.099								[23]
NaAlH ₄	0.75	5.60 %	6.7	69.4	1.24	89.3	0.072	-39.9	-120.7	16.5%	-99.1	497	58	2.0E-01	[24, 25]
NaAlH ₄ +TiCl ₃	0.75	5.03 %	6.0	66.0	1.31	99.5	0.076								
with tank	1.00	3.34 %	4.0	31.7		149.5	0.158								[13]
MOFs etc, min	1.00							-4.0		1.7%	-9.9	50	-213	1.2E+06	[13]
max	1.00							-10.0		4.1%	-24.8	125	-123	1.1E+05	[13]
LaNi ₅ H _{6.7}	1.00	1.54 %	1.8	101.5	6.60	325.1	0.049	-30.1	-109.3	12.5%	-74.8	375	3	2.7E+00	[26, 27]
Mg ₂ NiH ₄	1.00	3.62 %	4.3	93.1	2.57	138.1	0.054	-67.2	-122.0	27.8%	-166.7	837	278	4.0E-06	[28, 29]
MgH ₂	1.00	7.66 %	9.2	111.1	1.45	65.3	0.045	-75.7	-132.3	31.3%	-187.8	943	299	4.4E-07	[30, 31]
MgTiH ₄	1.00	5.29 %	6.3	148.9	2.82	94.5	0.034	-110.0	-132.0	45.5%	-272.9	1370	561	4.1E-13	[32]
TiH ₂	0.98	3.94 %	4.7	148.1	3.76	126.9	0.034	-144.3	-131.7	59.7%	-358.0	1798	823	3.9E-19	[33, 34]
LiBH ₄	0.75	13.88 %	16.7	91.6	0.66	36.0	0.055	-66.5	-97.8	27.5%	-165.1	829	407	2.8E-07	[34, 35]
NaBH ₄	1.00	10.66 %	12.8	118.3	1.11	46.9	0.042	-95.9	-108.6	39.7%	-237.9	1194	610	7.4E-12	[36, 37]
2LiBH ₄ +MgH ₂	0.80	11.54 %	13.8			43.3		-45.8	-104.3	19.0%	-113.7	571	166	2.6E-03	[31, 34]
2LiBH ₄ +AlH ₃	0.82	12.33 %	14.8			40.5		-32.0	-107.2	13.2%	-79.4	399	26	9.8E-01	[31, 34, 38]
2LiBH ₄ +TiH ₂	0.80	8.63 %	10.4			58.0		-16.1	-102.8	6.7%	-40.0	201	-116	3.5E+02	[34, 39]
2NaBH ₄ +MgH ₂	0.80	7.91 %	9.5			63.2		-63.7	-101.2	26.3%	-157.9	793	356	1.4E-06	[31, 34, 37]
2NaBH ₄ +TiH ₂	0.80	6.42 %	7.7			77.9		-33.9	-99.7	14.0%	-84.2	423	67	1.8E-01	[31, 37, 39]
2NaBH ₄ +VH ₂	0.80	6.27 %	7.5			79.8		-27.1	-103.5	11.2%	-67.2	337	-11	4.6E+00	[37, 39, 40]

Table 2: Presentation of the hydrogen storage characteristics for some common hydrogen storage materials: pressurized gaseous hydrogen (GH₂), liquid hydrogen (LH₂), metal organic frameworks (MOFs,) and several metal hydrides.

All data for densities and standard enthalpies and entropies of formation as well as some data for the pure gaseous and liquid hydrogen (energy loss, energy and volumetric density) are taken from the literature. The other values are calculated using the formulae and values given in section 2 assuming boride formation for the borohydride – metal hydride mixtures and metal formation otherwise. Tank volume and heat production are calculated for 5 kg hydrogen corresponding to a cruising range of 480 km for the parameters assumed in Table 1. DOE targets for volumetric and gravimetric requirements are shown for comparison.

3. Results and Discussion

3.1 General results

A striking result is that enormous amounts of nitrogen would be needed to cool the tank during hydrogen uptake for practically all solid state materials investigated (see Table 2). That makes on-board refilling an unpractical solution, unless a better cooling procedure will be found. Therefore, the solution of off-board refilling as suggested by Løvvik [18] is clearly preferable.

The concept of off-board hydrogen refilling has implications for the choice of the best storage material. The properties of hydrogen uptake (hydrogenation temperature, pressure and dynamics) are of minor importance for this method; instead, easy hydrogen release at moderate temperature and good cycling performance are now the key issues. For the former one, 30 to 40 kJ/mol enthalpy difference is the ideal value. Therefore, we have collected data about the main classes of hydrogen storage material.

The values for different parameters of hydrogen storage materials shown in Table 2 are obtained by calculations as described in section 2 based on literature values for basic properties. Volumetric and gravimetric densities are calculated for the pure hydrogen storage material and in the case of compressed gas plus its container. Data of this high pressure vessel are taken from the literature [13]. The energy loss, theoretical desorption temperature and dehydrogenation pressure were calculated as described in section 2.

Table 2 shows these parameters for the most common storage methods i.e. hydrogen under high pressure, liquid nitrogen at -253°C as well as for solid state storage materials: metal organic frameworks (MOFs), some metal hydrides like $\text{LaNi}_5\text{H}_{6.7}$ and MgH_2 and for some complex hydrides (NaAlH_4 , LiBH_4 , NaBH_4). DOE (Department of Energy) target values are also presented [22].

Additional information about hydrogen release and uptake as well as information about the cycling stability are taken from the literature. They were added in order to show the performance of the substance as a hydrogen storage material (see Table 3).

It is obvious that the target values by the DOE cannot be reached by using compressed gas, neither for the gravitational nor for the volumetric density. Liquid hydrogen fulfills these requirements as well, but has significant drawbacks as discussed above. On the other hand, many of the solid state materials comply with these requirements (see Table 2).

Some metal hydrides like $\text{LaNi}_5\text{H}_{6.7}$ work very well, but have one serious drawback: the low gravimetric density.

Therefore, we will focus on three other options, complex hydrides (section 3.2), combining borohydrides with metal hydrides (section 3.3) and magnesium-titanium mixtures (section 3.4).

Material	dehydrogenation		uptake rate	hydrogenation		cycling	references
	release rate	temp [°C]		pressure [bar]	temp [°C]		
LaNi ₅ H ₆	quite fast	<100	fast	20 - 50	25	ok	[26]
Mg ₂ NiH ₄	fast	280	fast	10 - 20	200 - 300	good	[28, 41]
MgH ₂	slow	460	slow	50	350 - 400	good	[42]
nano-Mg	fast	200 - 280	fast	8	280	good	[42-45]
TiH ₂	fast	100 - 800	ok	30	100 - 800	ok	[46]
NaAlH ₄ + cat	ok	40 / 120	ok	50 - 160	50 - 170	good	[47]
LiBH ₄ + cat	ok	250 / 450	ok	155	600	?	[48, 49]
NaBH ₄	fast	475				unknown	[50]
2LiBH ₄ +MgH ₂	fast / slow	390 / 430	fast	50	250 - 300	good	[51]

Table 3: Hydrogen storage performance of different hydrogen storage materials:

Temperatures needed for hydrogenation uptake and release as well as the hydrogenation pressure are listed. In addition, the reaction rates, cycling properties are noted. Bold numbers mark values that are fine only for off-board refilling

3.2 Complex hydrides

The complex hydrides show high gravimetric and volumetric density, but have to be operated at high pressures and temperatures. The pressures are usually below 200 bar and can still be handled, but the high temperatures are an obstacle: the dehydrogenation temperature should not be higher than the operating temperature of the fuel cell (about 100°C) and hydrogenation should be possible at ambient temperatures for on-board refilling, which is not the case for any light hydrogen storage materials. Using off-board refilling reduces the obstacles significantly: pressures up to 200 bar and process temperatures of a few hundred degrees should not be a problem for a dedicated fixed charging station. This allows hydrogenation of most possible hydrogen storage materials of high gravimetric density (see Table 3). The release rate of the hydrogen does not need to be high and can usually be improved by catalysts of usage or nanomaterials [52, 53]. So, there are only 2 prerequisites left to fulfill: a significantly low desorption temperature and good cycling stability.

In this regard, doped NaAlH₄ is a good hydrogen storage material. It can reversibly store and release 4% hydrogen without loss over 35 cycles [52], and a proper choice of the catalyst

allowed reducing the desorption temperature to about 40°C for the first and 120°C for the second step [47, 52], i.e. below and close to the operating temperature of a fuel cell.

In off-board refilling, an even better capacity can be expected, because with sufficient pressure, temperature and time, 100% hydrogenation can always be reached [54]. As a consequence, the search for the ideal catalyst can then be concentrated on a fast and preferably complete hydrogen release at low temperatures. 5% reversible storage seems realistic, especially if only the catalyst is added, i.e. for instance Ti instead of TiCl_3 (cf. Table 2).

In a recent comparison [23] NaAlH_4 was found to have inferior performance compared to other hydrogen storage methods. However, our approach of refilling at the petrol station reduces the shortcomings:

The metal foam in the tank is needed for heat transport during the fast hydrogen absorption in the car, where up to 1 MW can occur [55]. Filling outside the car allows slow hydrogenation that can be adapted to the heat transport in the tank. The small units (used for the exchange) will facilitate hydrogen desorption. So the tank can be built with a smaller and simpler charge-discharge-system leading to a lighter tank.

We assume that the second dehydrogenation step will be used in the vehicle as well, though the temperature needed is above the working temperature of present high-temperature membrane fuel cells. This will again reduce mass and volume of the tank. If an adaption to the NaAlH_4 release temperature is not possible, the medium has to be heated for the last step. This will reduce the onboard efficiency, but waste heat of the fuel cell can be still be used for 2/3 of the hydrogen to be released.

In contrast to other storage materials, the effective transport via pipeline can be used. Compared to compressed hydrogen, no compressor is needed at the filling, because the filling can be performed with the pressure available in the pipeline system. These advantages lead to a low price (see below) and CO_2 emission compared to other methods [23]. Additionally, this system has low hydrogen loss.

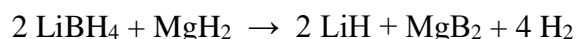
There remains the drawback of low desorption rate, which reduces the usable capacity of the tank [55]. This needs to be improved by new studies of this hydrogen storage material to further reduce volume and mass of the tank. With all these improvements in place, we think that the tank need not exceed 50 kg, which is still higher than a tank assumed for AlH_3 [56]. And with 5 mass% recyclable capacity, the material weighs another 100 kg.

Though NaAlH_4 is the most promising candidate for an application as hydrogen storage material, there are several other compounds, many of them with potentially higher storage

capacity, which might be used instead: other alanates (e.g. LiAlH_4), borohydrides (e.g. LiBH_4 or $\text{Al}(\text{BH}_4)_3$) or mixed alanates or borohydrides.

3.3 Mixtures of complex hydrides and metal hydrides

The thermodynamics of the complex hydrides could be meliorated by adding metal hydrides to change the chemical reaction, usually described as destabilization of the reactive hydride composites [51, 57, 58]. These composites show a lower heat production than the individual materials, which is caused by the stable product MgB_2 :



An additional advantage is the lack of borane formation, which appears if LiBH_4 is used alone [59, 60]. Unfortunately, the enthalpy difference is still higher than wanted. However, this led to the idea that a proper combination of a complex and a binary hydride could have the ideal properties for a hydrogen storage material. So Siegel *et al.* performed DFT calculations for 25 combinations of LiBH_4 or $\text{Ca}(\text{BH}_4)_2$ with various hydrides, evaluated the results, and found some combinations with the desired properties [61]. Some of their suggestions were tested afterwards, but a proper combination has not been obtained yet.

Gennari *et al.* investigated the system $\text{LiBH}_4 + \text{YH}_3$ and found that the size of the MH_x nano-particles (mechano-chemically obtained nanostructure) is one of the critical factors affecting the reaction of the hydride composites [53, 62]. MH_x nano-particles can also have a positive influence on the kinetics of the dehydrogenation of LiBH_4 [53].

We follow the approach of combining complex hydrides and metal hydrides by considering LiBH_4 and NaBH_4 as possible complex hydrides. This first analysis is restricted to considering enthalpies and entropies of formation. Table 3 summarizes these values for the most promising of these reactive composites of complex borohydrides and binary hydrides such as $\text{LiBH}_4 + \text{MgH}_2$.

A surprising result is that these values for the enthalpy differences differ quite significantly from those obtained by Siegel *et al.* [61]. For $\text{LiBH}_4 + \text{MgH}_2$, our value (45.8 kJ/mol) agrees much better with the value measured by Vajo and Skeith (42 kJ/mol) [57] than their results (50.4 kJ/mol). According to our calculations, 3 compositions are in the ideal range close to 30 kJ/mol: $\text{LiBH}_4 + \text{AlH}_3$, $\text{NaBH}_4 + \text{TiH}_2$, and $\text{NaBH}_4 + \text{VH}_2$. They are planned to be tested experimentally.

The approach of off-board refilling makes hydrogenation of $\text{LiBH}_4 + \text{MgH}_2$ easily applicable, in contrast to on-board refilling, where the hydrogenation temperature of 250°C to 300°C is higher than wanted (see Table 3). The only obstacle left for a practical use is the high desorption temperature. This is due to the high binding energy of the hydride. As the binding energies of the other compositions are lower, there is good hope that this parameter is also in a proper range for at least one of these composites.

3.4 Mixtures of magnesium and titanium hydride

One of the profoundly studied hydrogen storage material types is MgH_2 due to its low cost, high pressure, non-toxicity and abundance [41, 63]. From Table 2 it is visible that MgH_2 fulfills the DOE target for high gravimetric capacity (7,66 %) [64] and very good cycling stability. Unfortunately, the on-board usage of the above-mentioned properties is still impeded by its high stability (enthalpy of formation -75kJ/mol H_2), desorption temperature of about 300°C and poor hydrogenation and dehydrogenation kinetics [65].

It is experimentally proven that MgH_2 can be destabilized and the kinetics can be improved with the help of Ti as a catalyst [42, 66, 67]. Additionally, a first principle study shows thermodynamic destabilization of MgH_2 when Ti replaces partially Mg in the hydride, indicating that the desired value of enthalpy of formation can be achieved [68].

These two metals are not miscible and mechanical alloying is used for extending the solid solubility [69, 70]. Ti solubility in Mg is achieved [71] but the composite sometimes remains stable at temperatures below 250°C and the hydrogenation process facilitates the decomposition into MgH_2 and TiH_2 [71]. Other groups have obtained most rapid absorption at rather low temperature of 30°C and moderate pressure. The enthalpy and entropy of some Ti-mixed MgH_2 were not changed, but the activation energy was significantly reduced [67, 72] .

Several other groups reported rather similar results about different Mg-Ti ratio synthesized by reactive ball-milling under high hydrogen pressure [73-75]. Stability of those composites remains, but significant improvement of the sorption kinetics at lower temperatures is proved and hydrogen absorption at relatively low temperatures is achieved. The faster hydrogenation reaction of the composites at lower temperature is fully applicable for filling of the fuel tank outside the vehicles.

Titanium hydride forms at ambient pressures and temperatures and those properties allow using Ti-alloys as negative electrode in NiMH batteries [76]. Once formed, titanium hydride remains stable up to 450 - 600°C [77]. In order to be used as a negative electrode the Ti-hydride

is destabilized and multi-phase alloys as TiFe and TiNi mixed by other additives are used in practice [76].

Thermodynamic destabilization of those composites is achieved by Anastasopol *et al.* [78]; other authors have obtained good cycling stability and kinetic results on the MgH₂-TiH₂ system synthesized by reactive mechanical milling [74, 79-82]. Hydrogen capacity remains over 5 cycles between 4.82 and 5.91 wt.% in a temperature range from 126°C to 313°C [80]. Lu *et al.* obtained a nanostructured MgH₂-0.1TiH₂ composite with very good sorption kinetics and very high stability on reversible hydrogen sorption over 80 cycles [83]. The values of enthalpy and entropy of formation are estimated to be 69.8 kJ/mol H₂ and 129 J/(K mol H₂).

The effect of TiH₂ on the kinetic properties of MgH₂ is attributed mainly to its catalytic effect. Ponthieu *et al.* confirm that TiH₂ limits the grain growth of Mg and MgH₂ phases shortening the diffusion paths and H-mobility through existence of coherent coupling between TiH₂ and Mg/MgH₂ phases. The TiH₂ phase acts as gateway for hydrogen sorption even in the presence of MgO. This facilitates the abundant nucleation for the Mg and MgH₂ phases. The cycling of the nanocomposite is stable over 100 cycles [82, 84].

Good material durability of magnesium titanium composites makes them very promising candidates for hydrogen storage media. Slow hydrogenation lower temperatures fits quite well to the idea of charging replaceable tanks outside vehicles. Further investigation about the exact ratio between Mg and Ti has to be performed as well as extensive studies about the reaction mechanism.

3.6 Price considerations

While the weight of a NaAlH₄ tank is higher compared to a Type 4 compressed gas tank, it has advantages in terms of costs. Ahluwalia *et al.* found it one of the cheapest of all solutions with a price per km of only 0.11 \$/km compared to 0.10 \$/km for a combustion engine in the USA [23]. In Europe with significantly higher petrol prices it would be even cheaper than petrol.

Furthermore, there are good conditions for hydrogen production in Europe: electricity is generated to a high degree from solar and wind energy. As a consequence, electricity prices vary a lot. On sunny and windy summer days, the price even becomes negative in parts of central Europe due to limitations in pump storage and transport capacities. With a rising fraction of wind and solar energy in the electricity generation, this effect becomes more and more pronounced. Therefore, hydrogen can be produced for a low price from natural resources, if the

production is concentrated to times of excess supply of electricity. Such a hydrogen production will also allow to further extent the electricity generation from wind and sun.

3.6 Possible applications

Off-board refilling allows using the heat generated during hydrogenation in a useful way, either for thermolysis of hydrogen as suggested by Løvvik [18], for heating in the surrounding of the filling station or for electricity production, e.g. by use of thermoelectrics. It has the additional advantage of a short refilling time. Off-board refilling would allow hydrogenation at high pressures and temperatures, thus reducing the requirements for the hydrogen storage material significantly.

Standardized containers of 10 to 15 kg might be used, which could serve small and large vehicles with the same units; and they would allow refilling the fuel before all hydrogen is used up. They can also be a good option for plug-in hybrid cars.

It is worth noticing that the weight of the complete tank including the fuel cell is more than a factor of 2 lower for compressed hydrogen compared to the best Li-ion batteries available today for a long cruising range; using solid state hydrogen materials, this can be improved by another factor of 1.5 (see Table 1b, cf. [6]).

As shown in Table 1 and discussed in section 2.3, an electric car using a battery is the best solution for cars, mainly meant to be used in the city. For cars used for long distances, the electro cars are less advantageous because they will be very heavy and refilling on the way becomes an obstacle. For this purpose, hydrogen cars are the better solution.

4. Conclusion

While electric cars usually have the lowest primary energy consumption for short ranges, it is minimal for hydrogen cars for long cruising ranges, if losses due to storage of electricity and/or energy needed to produce the car are taken into account. Therefore, the development of all parts of hydrogen cars need further development. Due to the drawback of both hydrogen storage methods, compressed gas and liquid hydrogen, it is worth continuing to search for good solid state materials for hydrogen storage. On board refilling of solid state hydrogen storage materials is prevented by the enormous amount of liquid nitrogen needed for cooling. Therefore off-board refilling is the only solution. It enables short refilling times and the use of excess heat

(instead of expensive and complicated cooling). It reduces the requirements for hydrogen storage materials (by allowing high temperatures and pressures for hydrogenation) and shows promise to higher reversible hydrogen storage capacities (of the same material), so that the DOE requirements can be fulfilled by materials like NaAlH_4 or Mg-Ti composites. Other alanates, borohydrides and composites of borohydrides and metal hydrides have the potential for even better performance as hydrogen storage materials.

5. Acknowledgement

The authors would like to thank the Northern-Norway Research Council for financial support (pre-project 238664) in performing this study.

6. References

1. *Climate change 2013: The Physical Science Basis, Working Group 1 Contribution to the 5th Assessment report of the IPCC*. 2014, Cambridge University Press. p. 166.
 2. Stips, A., et al., *On the causal structure between CO₂ and global temperature*. Scientific Reports, 2016. **6**: p. 21691.
 3. El-Guebaly, L.A., *Fifty Years of Magnetic Fusion Research (1958–2008): Brief Historical Overview and Discussion of Future Trends*. Energies, 2010. **3**(6).
 4. Bartle, A., *Hydropower potential and development activities*. Energy Policy, 2002. **30**(14): p. 1231-1239.
 5. Rybach, L., *Geothermal Power Growth 1995–2013—A Comparison with Other Renewables*. Energies, 2014. **7**(8).
 6. Thomas, C.E., *Fuel cell and battery electric vehicles compared*. International Journal of Hydrogen Energy, 2009. **34**(15): p. 6005-6020.
 7. Marjanovic, I., et al. *Influence of Power-to-Gas-technology on unit commitment and power system operation*. in *2017 6th International Conference on Clean Electrical Power (ICCEP)*. 2017.
 8. de Boer, H.S., et al., *The application of power-to-gas, pumped hydro storage and compressed air energy storage in an electricity system at different wind power penetration levels*. Energy, 2014. **72**: p. 360-370.
 9. Yang, C.-J., *Chapter 2 - Pumped Hydroelectric Storage*, in *Storing Energy*, T.M. Letcher, Editor. 2016, Elsevier: Oxford. p. 25-38.
 10. Weidenthaler, C. and M. Felderhoff, *Solid-state hydrogen storage for mobile applications: Quo Vadis?* Energy & Environmental Science, 2011. **4**(7): p. 2495-2502.
 11. Venter, R.D. and G. Pucher, *Modelling of stationary bulk hydrogen storage systems*. International Journal of Hydrogen Energy, 1997. **22**(8): p. 791-798.
 12. Züttel, A., *Hydrogen storage methods*. Naturwissenschaften, 2004. **91**(4): p. 157-172.
 13. Eberle, U., M. Felderhoff, and F. Schuth, *Chemical and Physical Solutions for Hydrogen Storage*. Angewandte Chemie-International Edition, 2009. **48**(36): p. 2-25.
 14. Peters, J.F., et al., *The environmental impact of Li-Ion batteries and the role of key parameters – A review*. Renewable and Sustainable Energy Reviews, 2017. **67**: p. 491-506.
 15. E. Helmers, M.W., *Advances and Critical Aspects in the Life-Cycle Assessment of Battery Electric Cars*. Energy and Emission Control Techniques 2017. **5**: p. 1-18.
 16. https://www.energy.gov/sites/prod/files/2014/03/f12/fctt_pemfc_cost_review_0908.pdf.
 17. B.D.James, C.H., J.M. Huya-Kouadio, D.A.DeSantis, *Final Report:hydrogen Storage System Cost Analysis*. 2016.
 18. Løvvik, O.M., *Viable storage of hydrogen in materials with off-board recharging using high-temperature electrolysis*. International Journal of Hydrogen Energy, 2009. **34**(6): p. 2679-2683.
 19. Niaz, S., T. Manzoor, and A.H. Pandith, *Hydrogen storage: Materials, methods and perspectives*. Renewable and Sustainable Energy Reviews, 2015. **50**: p. 457-469.
 20. von Helmolt, R. and U. Eberle, *Fuel cell vehicles: Status 2007*. Journal of Power Sources, 2007. **165**(2): p. 833-843.
 21. Zhang, Y., J.R.G. Evans, and S. Yang, *Corrected Values for Boiling Points and Enthalpies of Vaporization of Elements in Handbooks*. Journal of Chemical & Engineering Data, 2011. **56**(2): p. 328-337.
 22. <https://www.energy.gov/eere/fuelcells/hydrogen-storage>. DOE
- Available from: <http://energy.gov/eere/fuelcells/hydrogen-storage>.
23. Ahluwalia, R.K., T.Q. Hua, and J.K. Peng, *On-board and Off-board performance of hydrogen storage options for light-duty vehicles*. International Journal of Hydrogen Energy, 2012. **37**(3): p. 2891-2910.

24. Šubrtova, V., *Röntgenographische Studie des Isotopeneffektes an Kristallen einfacher und komplexer Hydride*. Zeitschrift für anorganische und allgemeine Chemie, 1967. **350**(3-4): p. 211-213.
25. Lee, B.-M., et al., *Thermodynamic assessment of the $\text{NaH} \leftrightarrow \text{Na}_3\text{AlH}_6 \leftrightarrow \text{NaAlH}_4$ hydride system*. Journal of Alloys and Compounds, 2006. **424**(1): p. 370-375.
26. J.H.N. van Vucht, F.A.K., H.C.A.M. Burning, *Reversible room-temperature absorption og large quantities of hydrogen by intermetallic compounds*. Philips Res.Rep., 1970. **25**: p. 133-140.
27. Mendelsohn, M.H., D.M. Gruen, and A.E. Dwight, *$\text{LaNi}_5\text{-xAlx}$ is a versatile alloy system for metal hydride applications*. Nature, 1977. **269**: p. 45.
28. Reilly, J.J. and R.H. Wiswall, *Reaction of hydrogen with alloys of magnesium and nickel and the formation of Mg_2NiH_4* . Inorganic Chemistry, 1968. **7**(11): p. 2254-2256.
29. Zeng, K., et al., *Thermodynamic analysis of the hydriding process of Mg–Ni alloys*. Journal of Alloys and Compounds, 1999. **283**(1): p. 213-224.
30. Ellinger, F.H., et al., *The Preparation and Some Properties of Magnesium Hydride*1. Journal of the American Chemical Society, 1955. **77**(9): p. 2647-2648.
31. Glushko Thermocenter of the Russian Academy of Science, I.A., Izorskaya 13/19, 127412 Moscow, Russia (1994)
32. Rousselot, S., D. Guay, and L. Roué, *Synthesis of fcc Mg–Ti–H alloys by high energy ball milling: Structure and electrochemical hydrogen storage properties*. Journal of Power Sources, 2010. **195**(13): p. 4370-4374.
33. Yakel, H., Jnr, *Thermocrystallography of higher hydrides of titanium and zirconium*. Acta Crystallographica, 1958. **11**(1): p. 46-51.
34. M.W.Chase, *JANAF Thermochemical Data*. Journal of Physical and Chemical Data. Vol. 14, supp.no1 1985.
35. Harris, P.M. and E.P. Meibohm, *THE CRYSTAL STRUCTURE OF LITHIUM BOROHYDRIDE LiBH_4* . Journal of the American Chemical Society, 1947. **69**(5): p. 1231-1232.
36. Babanova, O.A., et al., *Structural and Dynamical Properties of NaBH_4 and KBH_4 : NMR and Synchrotron X-ray Diffraction Studies*. The Journal of Physical Chemistry C, 2010. **114**(8): p. 3712-3718.
37. THERMODATA, G.C., 1001 Avenue Centrale, BP 66, F-38042 Saint Martin d'Hères, France (1994).
38. I. Barin, O.K., *Thermochemical Properties of Inorganic Substances*. 1973+Supplement (1977), Düsseldorf Springer Verlag Berlin and Verlag Stahleisen mbH.
39. SGTE, G.C., 1001 Avenue Centrale, BP 66, F-38042 Saint martin d'Hères, France (1994).
40. Golubkov, A.N. and A.A. Yukhimchuk, *High-Pressure Hydrogen Isotopes Sources Based on Vanadium Hydride*. Hyperfine Interactions, 2001. **138**(1): p. 403-408.
41. Sakintuna, B., F. Lamari-Darkrim, and M. Hirscher, *Metal hydride materials for solid hydrogen storage: A review*. International Journal of Hydrogen Energy, 2007. **32**(9): p. 1121-1140.
42. Zaluska, A., L. Zaluski, and J.O. Ström–Olsen, *Nanocrystalline magnesium for hydrogen storage*. Journal of Alloys and Compounds, 1999. **288**(1–2): p. 217-225.
43. M. Khrussanova, M.T., P. Peshev, I. Konstanchuk, E. Ivanov, Z. Phys. Chem. (N.F.), 1989. **164**: p. 1261-1266.
44. Dornheim, M., et al., *Hydrogen storage in magnesium-based hydrides and hydride composites*. Scripta Materialia, 2007. **56**(10): p. 841-846.
45. Wagemans, R.W.P., et al., *Hydrogen Storage in Magnesium Clusters: Quantum Chemical Study*. Journal of the American Chemical Society, 2005. **127**(47): p. 16675-16680.
46. Suwarno, S. and V.A. Yartys, *Kinetics of Hydrogen Absorption and Desorption in Titanium*. 2017, 2017: p. 6.
47. Bogdanović, B., et al., *Metal-doped sodium aluminium hydrides as potential new hydrogen storage materials*. Journal of Alloys and Compounds, 2000. **302**(1): p. 36-58.
48. Züttel, A., et al., *LiBH_4 a new hydrogen storage material*. Journal of Power Sources, 2003. **118**(1–2): p. 1-7.

49. Maunon, P., et al., *Stability and Reversibility of LiBH₄*. The Journal of Physical Chemistry B, 2008. **112**(3): p. 906-910.
50. Urgnani, J., et al., *Hydrogen release from solid state NaBH₄*. International Journal of Hydrogen Energy, 2008. **33**(12): p. 3111-3115.
51. Bösenberg, U., et al., *Hydrogen sorption properties of MgH₂-LiBH₄ composites*. Acta Materialia, 2007. **55**(11): p. 3951-3958.
52. Bogdanović, B. and M. Schwickardi, *Ti-doped alkali metal aluminium hydrides as potential novel reversible hydrogen storage materials*¹. Journal of Alloys and Compounds, 1997. **253-254**: p. 1-9.
53. Cai, W., et al., *Nanosize-Controlled Reversibility for a Destabilizing Reaction in the LiBH₄-NdH_{2+x} System*. The Journal of Physical Chemistry C, 2013. **117**(19): p. 9566-9572.
54. Dymova T. N., E.N.G., Bakum S. I. and Dergachev Yu.M. , *Direct Synthesis of alkale metal aluminium hydrides in the melt*. Dokl.Akad. Nauk SSSR, 1975. **2015**: p. 256-259.
55. Ahluwalia, R.K., *Sodium alanate hydrogen storage system for automotive fuel cells*. International Journal of Hydrogen Energy, 2007. **32**(9): p. 1251-1261.
56. Ahluwalia, R.K., T.Q. Hua, and J.K. Peng, *Automotive storage of hydrogen in alane*. International Journal of Hydrogen Energy, 2009. **34**(18): p. 7731-7740.
57. Vajo, J.J., S.L. Skeith, and F. Mertens, *Reversible Storage of Hydrogen in Destabilized LiBH₄*. The Journal of Physical Chemistry B, 2005. **109**(9): p. 3719-3722.
58. Alapati, S.V., J.K. Johnson, and D.S. Sholl, *Predicting Reaction Equilibria for Destabilized Metal Hydride Decomposition Reactions for Reversible Hydrogen Storage*. The Journal of Physical Chemistry C, 2007. **111**(4): p. 1584-1591.
59. Jaron, T. and W. Grochala, *Y(BH₄)₃-an old-new ternary hydrogen store aka learning from a multitude of failures*. Dalton Transactions, 2010. **39**(1): p. 160-166.
60. Jeon, E. and Y. Cho, *Mechanochemical synthesis and thermal decomposition of zinc borohydride*. Journal of Alloys and Compounds, 2006. **422**(1): p. 273-275.
61. Siegel, D.J., C. Wolverton, and V. Ozoliņš, *Thermodynamic guidelines for the prediction of hydrogen storage reactions and their application to destabilized hydride mixtures*. Physical Review B, 2007. **76**(13): p. 134102.
62. Gennari, F.C., *Improved hydrogen storage reversibility of LiBH₄ destabilized by Y(BH₄)₃ and YH₃*. International Journal of Hydrogen Energy, 2012. **37**(24): p. 18895-18903.
63. Jain, I.P., C. Lal, and A. Jain, *Hydrogen storage in Mg: A most promising material*. International Journal of Hydrogen Energy, 2010. **35**(10): p. 5133-5144.
64. Schlapbach, L. and A. Züttel, *Hydrogen-storage materials for mobile applications*. Nature, 2001. **414**(6861): p. 353-358.
65. Mintz, M.H., Z. Gavra, and Z. Hadari, *Kinetic study of the reaction between hydrogen and magnesium, catalyzed by addition of indium*. Journal of Inorganic and Nuclear Chemistry, 1978. **40**(5): p. 765-768.
66. Hanada, N., T. Ichikawa, and H. Fujii, *Catalytic Effect of Nanoparticle 3d-Transition Metals on Hydrogen Storage Properties in Magnesium Hydride MgH₂ Prepared by Mechanical Milling*. The Journal of Physical Chemistry B, 2005. **109**(15): p. 7188-7194.
67. Liang, G., et al., *Catalytic effect of transition metals on hydrogen sorption in nanocrystalline ball milled MgH₂-Tm (Tm=Ti, V, Mn, Fe and Ni) systems*. Journal of Alloys and Compounds, 1999. **292**(1): p. 247-252.
68. Song, Y., Z.X. Guo, and R. Yang, *Influence of titanium on the hydrogen storage characteristics of magnesium hydride: a first principles investigation*. Materials Science and Engineering: A, 2004. **365**(1): p. 73-79.
69. J.B., N.-H.A.A.a.C., *Phase Diagrams og Binary Magnesium Alloys*. 1988: ASM International, Metals Park, OH.
70. Yavari A.R., D.P.J.a.B.T., *Mechanically driven alloying of immisible elements*. Phys. Rev.Lett., 1992. **68**: p. 2235.

71. Liang, G. and R. Schulz, *Synthesis of Mg-Ti alloy by mechanical alloying*. Journal of Materials Science, 2003. **38**(6): p. 1179-1184.
72. Phetsinorath, S., et al., *Preparation and hydrogen storage properties of ultrafine pure Mg and Mg-Ti particles*. Transactions of Nonferrous Metals Society of China, 2012. **22**(8): p. 1849-1854.
73. Lu, W.-C., et al., *Hydriding characteristics of Mg-Ti alloys prepared by reactive mechanical grinding and hydrogen pulverization*. Journal of Alloys and Compounds, 2016. **664**(Supplement C): p. 193-198.
74. Shao, H., M. Felderhoff, and F. Schüth, *Hydrogen storage properties of nanostructured MgH₂/TiH₂ composite prepared by ball milling under high hydrogen pressure*. International Journal of Hydrogen Energy, 2011. **36**(17): p. 10828-10833.
75. Lu, C., et al., *Synthesis and hydrogen storage properties of core-shell structured binary Mg@Ti and ternary Mg@Ti@Ni composites*. International Journal of Hydrogen Energy, 2017. **42**(4): p. 2239-2247.
76. Kleperis, J., et al., *Electrochemical behavior of metal hydrides*. Journal of Solid State Electrochemistry, 2001. **5**(4): p. 229-249.
77. Manchester F.D. and Khatamian D., M.f.A.o.I.H.A., Materials Science Forum, Vol. 31, pp. 261-296, 1988, "Mechanisms for Activation of Intermetallic Hydrogen Absorbers". Materials Science Forum, 1988. **31**: p. 261-296.
78. Anastasopol, A., et al., *Reduced Enthalpy of Metal Hydride Formation for Mg-Ti Nanocomposites Produced by Spark Discharge Generation*. Journal of the American Chemical Society, 2013. **135**(21): p. 7891-7900.
79. Biasetti, A., M. Meyer, and L. Mendoza Zélis, *Hydriding kinetics of MgTiH₂ fine dispersions obtained by mechanosynthesis*. Powder Technology, 2017. **307**(Supplement C): p. 145-152.
80. Choi, Y.J., et al., *Hydrogen storage properties of the Mg-Ti-H system prepared by high-energy-high-pressure reactive milling*. Journal of Power Sources, 2008. **180**(1): p. 491-497.
81. Cuevas, F., D. Korablov, and M. Latroche, *Synthesis, structural and hydrogenation properties of Mg-rich MgH₂-TiH₂ nanocomposites prepared by reactive ball milling under hydrogen gas*. Physical Chemistry Chemical Physics, 2012. **14**(3): p. 1200-1211.
82. Ponthieu, M., et al., *Synthesis by reactive ball milling and cycling properties of MgH₂-TiH₂ nanocomposites: Kinetics and isotopic effects*. International Journal of Hydrogen Energy, 2014. **39**(18): p. 9918-9923.
83. Lu, J., et al., *Hydrogen Storage Properties of Nanosized MgH₂-0.1TiH₂ Prepared by Ultrahigh-Energy-High-Pressure Milling*. Journal of the American Chemical Society, 2009. **131**(43): p. 15843-15852.
84. Ponthieu, M., et al., *Structural Properties and Reversible Deuterium Loading of MgD₂-TiD₂ Nanocomposites*. The Journal of Physical Chemistry C, 2013. **117**(37): p. 18851-18862.
85. R.C.Weast, *Handbook of Chemistry and Physics* ed. th. 1974-1975, Cleveland, Ohio: CRC press
86. Wegrzyn, J. and M. Gurevich, *Adsorbent storage of natural gas*. Applied Energy, 1996. **55**(2): p. 71-83.

Appendix 1:

energy density of Li-ion batteries	0.875	MJ/kg	[6]
energy density H ₂	120.0	MJ/kg	[10]
energy density petrol	44.0	MJ/kg	[10]
energy density methane	50.0	MJ/kg	[85]
mass of battery for a FCEV	20.0	kg	estimated
mass of battery for car using combustion engine	15.0	kg	measured
mass of petrol tank	7.0	kg	estimated
ratio tank mass/fuel mass for methane	4.9		[86]
ratio tank mass/fuel mass for large CGH ₂ tank	16.5		[17]
ratio tank mass/fuel mass for small CGH ₂ tank	20.0		estimated
ratio tank mass/fuel mass for NaAlH ₄ hydrogen tank	50.0		estimated
recyclable H ₂ density in NaAlH ₄	0.050		calculated
fuel cell power per mass	0.694	kW/kg	[16]
usable capacity for Li ion batteries	0.700		[6]
efficiency of drive train using combustion engine	25.6%		[6, 20]
efficiency of drive train using electric motor	79.2%		[6]
pumped storage efficiency	75.0%		[9]
efficiency fuel cell	51.8%		[6]
efficiency methane->electricity by combined circle	48.0%		[6]
efficiency of H ₂ production from methane	75.0%		[6]
efficiency of H ₂ from electricity	75.0%		[6]
efficiency of H ₂ transport in pipeline	99.0%		calculated
efficiency of electricity transport	92.0%		[6]
efficiency of fuel transport by truck	99.0%		calculated
efficiency of battery charging	94.0%		[6]
efficiency of battery discharging	90.0%		[6]
Efficiency: H ₂ tank 850 bar	84.0%		[13]
Efficiency: H ₂ tank with NaAlH ₄	85.1%		calculated

Table A.1: List of technical data used for the calculation in this paper and their references